CORTICAL PROTON MR SPECTROSCOPIC IMAGING ABNORMALITIES IN A MACAQUE MODEL OF NEUROAIDS

William E. Wu[1], Assaf Tal[1], James S. Babb[1], Eva-Maria Ratai[2], R. Gilberto Gonzalez[2], and Oded Gonen[1]

[1]*Radiology, New York University School of Medicine, New York, New York, United States,* [2]*Neuroradiology, Massachusetts General Hospital, Athinoula A. Martinos Center for Biomedical Imaging, Charlestown, Massachusetts, United States*

TARGET AUDIENCE: HIV Clinicians. HIV/SIV Pathogenesis Researchers. MR Spectroscopy Researchers. The HIV-Infected Population.

PURPOSE: Even as highly-active antiretroviral therapy (HAART) reduces incidence of HIV-dementia, milder forms of HIV-associated neurocognitive disorders (HAND) continue to be a health concern due to complications from chronic infection[1]. Previous quantitative MRI studies have shown HIV-related thinning of the cerebral cortex (even amongst those receiving HAART), which correlated with $CD4^+$ T-lymphocyte depletion and cognitive deficits[2]. Multivoxel proton-MR spectroscopic imaging (^{1}H-MRSI) studies, however, have yet to examine substantial portions of cortex. We previously reported unchanged *N*-acetylaspartate (NAA) in the global gray matter[3] (GM) of simian immunodeficiency virus (SIV)-infected rhesus macaques, a well-established model system of HIV-infection. Prior histopathology, however, has revealed neuronal loss specifically in cortical regions[4]. (It is worth noting that our previous global analyses would have averaged out all regional changes.) Consequently, in this post hoc study we test the hypothesis that early cortical SIV-infection is characterized by: *(i)* neuronal damage, reflected by a decrease in their NAA concentration; and *(ii)* glial activation, marked by increased *myo*-inositol (*m*I), choline (Cho) and creatine (Cr)[5].

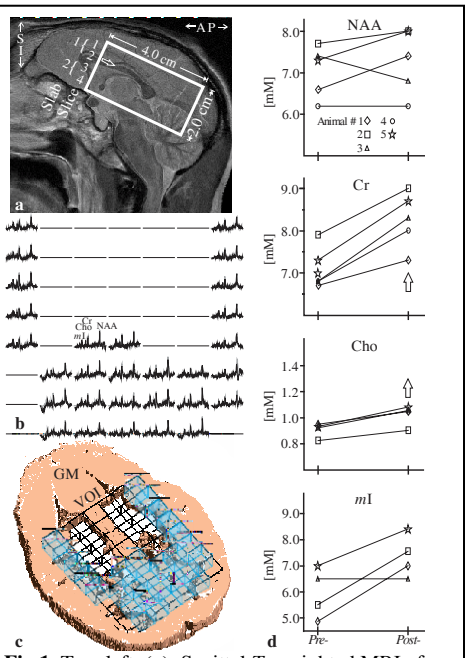

Fig 1. Top, left, (**a**): Sagittal T_2-weighted MRI of a rhesus macaque head 4 weeks *post*-SIV infection showing the 3.5×4×2 cm^3 VOI (solid lines) placement. Note the open arrow on **a** denotes the level of **b** and **c**. Middle, left, (**b**): Real part of the 7×8 (LR×AP) ^{1}H spectra matrix on common chemical shift and intensity scales. Note the SNR and spectral resolution in those $(0.5\ cm)^3$ =0.125 cm^3 voxels. Bottom, left, (**c**): 3D view of the cortical partial volumes (beige) in a ^{1}H-MRSI slice with voxels meeting the ≥90% total volume fraction threshold highlighted (blue). Note the absence of deep GM structures whose voxels' contents were excluded. Right, (**d**): Line-plots of the NAA, Cr, Cho and *m*I concentration changes from *pre*-to-*post* infection scans for each animal (denoted by symbols in the key). Note the statistically significant increases (open arrows) in mean Cr and Cho, as well as a near-significant elevation in *m*I.

METHODS: Five (two females; 5.0 to 8.6 kg weight) healthy 3-year-old rhesus macaques (*Macaca mulatta*) were scanned under constant veterinary supervision, as described elsewhere[3]. Each animal was then inoculated intravenously with SIV_{mac251} virus (10 ng SIVp27) and $CD8^+$ T-lymphocyte depleted with CD8-targeted (cM-T807) antibody[6]. Two animals were rescanned 4 weeks and three 6 weeks later. Scans were performed in a whole-body 3 T imager (Magnetom TIM Trio, Siemens AG, Erlangen, Germany) using its transmit-receive knee-coil. Sagittal and axial T_2-weighted turbo spin echo (TSE) MRI: *TE/TR* = 16/7430 ms were acquired. A 4.0 cm anterior-posterior (AP) ×3.5 cm left-right (LR) ×2.0 cm inferior-superior (IS) =28 cm^3 volume-of-interest (VOI) was then image-guided and excited with dual-slab PRESS (*TE/TR* =33/1440 ms; Fig. 1**a**). Relative NAA, Cr, Cho and *m*I levels in the VOI's 224 voxels – obtained with SIToolsFITT package[7] (Fig. 1**b**) – were scaled into absolute concentrations against a 0.5 L phantom of known concentrations, as described previously[3]. Since metabolite concentrations may vary among deep GM structures, cerebellum and cortex, we produced GM and white matter (WM) masks from the axial TSE images, as described elsewhere[3]. We then carefully erased the striatum, thalamus and cerebellum from GM masks based on a rhesus macaque brain atlas[8], keeping only voxels with ≥90% total (GM+WM) volume fraction, as shown in Fig. 1**c**. We then solved for the unknown "cortical" GM metabolites' concentrations in the remaining voxels with linear regression. Since five animals were insufficient for nonparametric tests of metabolic change, paired sample *t* tests were used to assess each metabolite's *pre*-to-*post*-infection change. Significance was tested at the $p<0.05$ level using SAS version 9.3 (SAS Institute, Cary, NC).

RESULTS: The ≥90% total voxel tissue constraint left approximately 450 "cortical" GM voxels (~90/animal ×5 animals) for analysis. Their metabolite SNRs were: NAA=25±8, Cr=16±6, Cho=10±3 and *m*I=10±4, which led to reliable voxel fits (all Cramer-Rao lower bounds ‹15%). Mean *pre*-to-*post* infection Cr increased 15% (7.2±0.4 to 8.3±0.7 mM, $p<0.05$); Cho 10% (0.9±0.1 to 1.0±0.1 mM, $p<0.01$); and *m*I 28% (5.8±0.9 to 7.4±0.8 mM, $p=0.06$), as shown in Fig. 1**d**. NAA was unchanged.

DISCUSSION: Increases in *m*I, a glia-specific marker[5], Cho and Cr reflect glial activation in cortex contained within the VOI. Elevated *m*I is consistent with previous neuropathology in this model[4], showing widespread elevations of glial fibrillary acidic protein and ionized calcium binding adaptor molecule 1 – an immunohistochemical marker of microglial activation – at four and eight weeks *post*-infection. Unchanged NAA, however, suggests neuronal cell bodies may be spared early on in the disease. One implication is that astrocyte/microglial activation may *precede* neuropathogenesis, consistent with evidence previously reported[3]. It is also possible that WM injury at first or alone may explain cognitive deficits observed[9]. It is noteworthy that due to presence of lipids the VOI was limited to midline/parietal cortex, ~20% of its total.

CONCLUSION: Taken together with previous findings[3], these results suggest treatment regimens to reduce gliosis may be helpful in preventing downstream neurodegeneration and cognitive impairment. Provided that further animal testing demonstrates safety, future HIV treatment regimens may benefit from anti-inflammatory drugs aimed at reducing gliosis as a possible therapeutic strategy against HAND.

REFERENCES: 1. Heaton RK, Franklin DR, Ellis RJ et al. HIV-associated neurocognitive disorders before and during the era of combination antiretroviral therapy: differences in rates, nature, and predictors. J Neurovirol. 2011;17:3-16

2. Thompson PM, Dutton RA, Hayashi KM et al. Thinning of the cerebral cortex visualized in HIV/AIDS reflects CD4+ T lymphocyte decline. Proc Natl Acad Sci U S A. 2005;102:15647-15652

3. Wu WE, Tal A, Kirov, II et al. Global gray and white matter metabolic changes after simian immunodeficiency virus infection in CD8-depleted rhesus macaques: proton MRS imaging at 3 T. NMR Biomed. 2013;26:480-488

4. Ratai EM, Annamalai L, Burdo T et al. Brain creatine elevation and N-Acetylaspartate reduction indicates neuronal dysfunction in the setting of enhanced glial energy metabolism in a macaque model of neuroAIDS. Magn Reson Med. 2011;66:625-634

5. Soares DP, Law M. Magnetic resonance spectroscopy of the brain: review of metabolites and clinical applications. Clin Radiol. 2009;64:12-21

6. Schmitz JE, Simon MA, Kuroda MJ et al. A nonhuman primate model for the selective elimination of CD8+ lymphocytes using a mouse-human chimeric monoclonal antibody. Am J Pathol. 1999;154:1923-1932

7. Soher BJ, Young K, Govindaraju V, Maudsley AA. Automated spectral analysis III: application to in vivo proton MR spectroscopy and spectroscopic imaging. Magn Reson Med. 1998;40:822-831

8. Frey S, Pandya DN, Chakravarty MM et al. An MRI based average macaque monkey stereotaxic atlas and space (MNI monkey space). Neuroimage. 2011;55:1435-1442

9. Gongvatana A, Schweinsburg BC, Taylor MJ et al. White matter tract injury and cognitive impairment in human immunodeficiency virus-infected individuals. J Neurovirol. 2009;15:187-195